Nanocomposite Polyvinyl Alcohol Fibers for Medical Applications

Teresa Mikołajczyk,[1] Stanisław Rabiej,[2] Maciej Boguń,[1] Grzegorz Szparaga,[1] Zbigniew Draczyński[3]

[1]*Departament of Man-Made Fibres, Technical University of Lodz, Lodz, Poland*
[2]*Department of Materials and Environmental Sciences, University of Bielsko-Biala, Bielsko-Biala, Poland*
[3]*Department of Physical Chemistry of Polymers, Technical University of Lodz, Lodz, Poland*

Received 11 December 2009; accepted 9 August 2010
DOI 10.1002/app.33233
Published online 9 November 2010 in Wiley Online Library (wileyonlinelibrary.com).

ABSTRACT: It was investigated how the HAp and SiO_2 nanoadditives introduced into the material of fibers made from polyvinyl alcohol (PVA) affects the structure, sorption, and strength properties of those fibers. The conditions of the fibers' production were selected with the aim of obtaining the nanocomposite PVA fibers which would be soluble in water and in body fluids. These fibers are intended to be used for the production of a biocomposite with another biodegradable polymer. The determination was made of the effect of two different deformations applied at the fiber production stage on the structure and properties of the fibers. Using the WAXS method, the supramolecular structure of the fibers was determined. Nanocomposite PVA fibers obtained in this work have an oriented crystalline structure with a rather low level of crystallinity, reaching 40%, and a relatively high orientation index of crystallites: 0.48–0.54. © 2010 Wiley Periodicals, Inc. J Appl Polym Sci 120: 1234–1244, 2011

Key words: nanocomposites; PVA fibers; hydroxyapatite; nanosilica

INTRODUCTION

The renaissance in the development of fibers made from polyvinyl alcohol (PVA) is linked principally to their medical applications.

In spite of the favorable sorption properties of such fibers, a limitation of their use in textiles is connected with their low-softening temperature, which makes textile products less convenient to use. However, the properties such as biodegradability, biocompatibility, and lack of toxicity have led to various medical applications.[1] It is also possible in that field to use PVA fibers produced with a modern electro-spinning method from 6 to 8% aqueous solutions.[2] The form of the nonwoven fabric with the nanometric diameter of the fibers in the range of 5–600 nm is such as to make the resulting material porous and enable it to be used for filtration and dressing materials. PVA fibers can be used not only in the form of surgical threads[3] but can also serve as a component of a new generation of implant materials. The implementation of ceramic nanoadditives such as hydroxyapatite (HAp) or tricalcium phosphate (TCP)[4,5] into the material of the fibers (as in the case of alginate fibers) will make it possible for implants containing them to be given osteoproductive and osteoconductive properties.

Fibers for use in textiles are as a rule produced with a classical wet-spinning solution method into a solidifying bath with high Na_2SO_4 content of around 300–400 g/L.[6] It is also possible to use the solutions of other salts of lower ion coagulability, according to the series: $SO_4^{2-} > CO_3^{2-} > {}_3COOH^- > C^- > NO_3^-$.[7]

The solidification of fibers may also take place in baths containing NaOH or in organic baths such as acetone or alcohol. However, the coagulability in this case is lower than in the case of inorganic baths.

Insolubility of fibers in hot water is achieved by crosslinking, primarily using formaldehyde (preceded by a drawing process).

The use of a method of dry spinning from solution[6] combined with the total draw ratio of 8–9 and technical treatment, or from a so-called semimelt also makes it possible to obtain fibers which are insoluble in hot water.[8] Their tenacity is around 90 cN/tex. These properties result from the high orientation of structural elements and the crystallinity of the material. Strength of the order of 0.9 GPa is obtained also using a gel formation method, to produce fibers from polymers with high-molecular masses.[9] However, in medical use, with the exception of surgical threads, high-strength properties are not necessary. It is important, on the other hand, that the fibers are free of residues of toxic solvents

Correspondence to: G. Szparaga (grzegorz.szparaga@gmail.com).

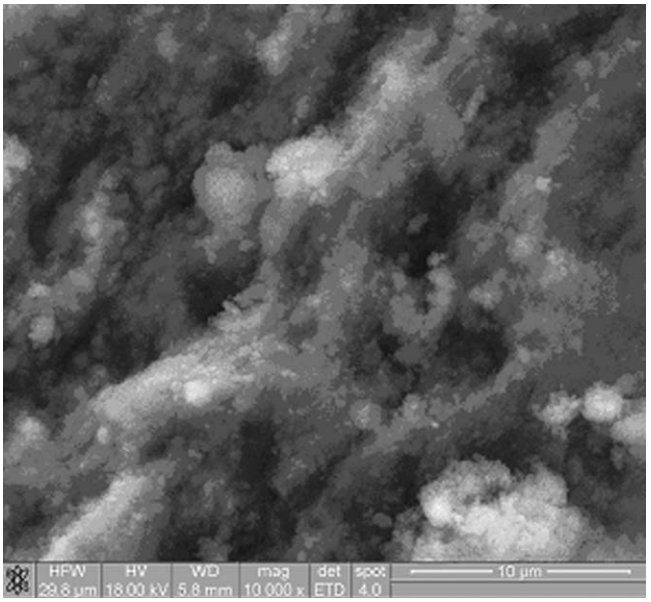

Figure 1 SEM image of hydroxyapatite.

or other ingredients of the solidifying baths, particularly when fibers are to be used in biocomposites. For this reason, it was decided to determine the conditions of the formation of PVA fibers with the wet-spinning solution method, while using suitable solutions of inorganic salts, which fulfill the above biocompatibility criteria, as solidifying baths.

The aim of this work was to determine the effect of the HAp or SiO_2 nanoadditives introduced into the material of PVA fibers on their structure and their sorption and strength properties.

From the point of view of the intended use of the fibers, it was sought to obtain two types of fibers differing in diameter (linear density). Their strength properties may be at a level sufficient for the production of a biocomposite material. These fibers will constitute an easily resorbable component of a biocomposite also containing a less easily resorbable polymer, such as poly ε-caprolactone. In this specific application of the fibers, high-strength properties are not even desirable, since they might reduce solubility. The good solubility of PVA fibers in body fluids also means that they will play the role of a pore-forming agent in the final implant material. The diameter of the fibers, their quantity, and their distribution in the biocomposite matrix will determine the nature of the porous structure, which controls the process of cell proliferation. Gradual release of HAp or SiO_2 nanoadditives can be expected to give the whole implant osteoproductive and osteoconductive properties.

The results of investigations of the degradation of biocomposites produced on the basis of nanocomposite PVA fibers in an artificial plasma environment will be the subject of a future publication.

MATERIALS AND METHODS

Description of the polymer, HAp, and SiO_2 nanoadditives and of the spinning solution

The spinning solution was prepared using polyvinyl alcohol (PVA) supplied by Sigma-Aldrich (St. Louis/Missouri), with molecular mass of 146.000–186.000, degree of polyvinyl acetate hydrolyzation: 99%. The intrinsic viscosity determined at 20°C was $[\acute{\eta}] = 1.1$ dcL/g.

In this work, the following nanoadditives, differing in chemical structure, specific surface, and particle size were used:

- Natural hydroxyapatite (HAp) $C_{10}(PO_4)_6(OH)$ obtained at the AGH University of Science and Technology (Kraków/Poland), according to patent.[10] Its specific surface as measured by the BET method was 73.6 m^2/g, and the average particle size was in the range of 100–800 nm (Fig. 1).
- Silica (SiO_2) was a commercial product from Sigma-Aldrich (St. Louis/Missouri). Its specific surface as measured by the BET method was 563.5 m^2/g, and average particle size was in the range of 60–100 nm (Fig. 2).

The nanoadditives were characterized by measuring their surface by a gas absorption method (BET), determination of particle size (DLS), and microscopic observation of the particles (SEM). Specific surface was measured with a Nova1200e apparatus from Quantachrome Inst. (Boynton Beach/Florida) using a BET absorption isotherm method. Particle size was determined with a Zetasizer Nano-ZS device from Malvern Inc. (Worcestershire/United Kingdom) using dynamic light scattering (DLS).

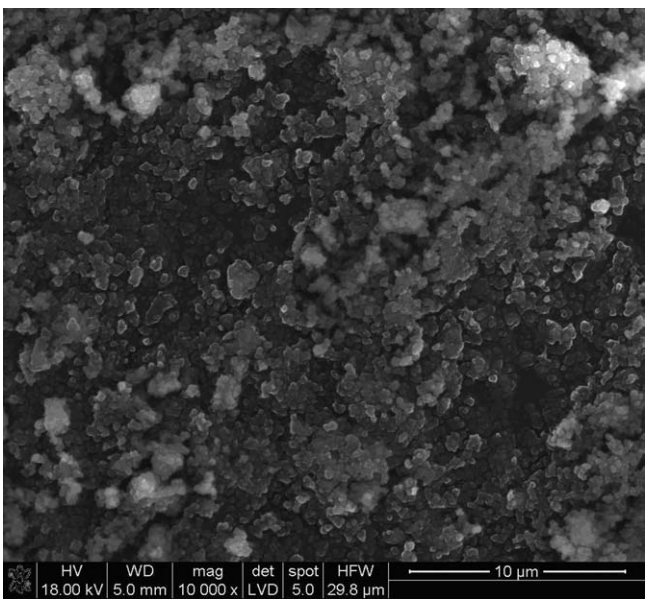

Figure 2 SEM image of silica.

Nanoadditives were added to the spinning solution in the form of a suspension in solvent during the preparation of the solution. To disperse the agglomerates, the suspension of nanoadditive was subjected to the action of ultrasounds, using a 100 W ultrasound probe, for 30 min at 20°C.

The solvent used for fiber formation was an 8% aqueous solution of urea. The addition of urea (a biocompatible substance) prevented the formation of hydrogen bonds in the solution between PVA macromolecules. The formation of secondary bonds with the NH_2 groups of urea prevented gelling of the spinning solution, ensuring its stability over the time required for filtration and deaeration. The concentration of the spinning solution was established, based on the preliminary tests, at such a level that the apparent dynamic viscosity was suitable for the formation of fibers with the wet spinning from solution method (it was within the range of 30 to 60 Pa s).

Rheological properties of the spinning solutions were determined using an Anton Paar (Graz/Austria) rotary rheometer. Measurements were made within a shearing rate ranged from 0.2 to 200×10^2 s^{-1} at a temperature of 20°C. The rheological parameters n and k were found from the flow curves.

Fiber formation

Fibers were formed using 13.2% spinning solutions of polyvinyl alcohol in a solvent (8% aqueous solution of urea). The content of the introduced nanoadditives was variable, amounting to 1%, 2%, or 3% in proportion to the polymer mass.

The fibers were formed with the wet spinning from solution method using a large laboratory spinning machine, having exchangeable modules, enabling the choice of configuration and offering a broad range of the process parameters. A 240-hole nozzle was used, with the hole diameter of 0.08 mm.

Solidification of the fibers took place in a saturated solution of NaCl at a temperature of 10°C. The solution was heated in a tank to a temperature of around 40–50°C.

To obtain two different linear density assortments, the fiber forming process was carried out at two different values of total deformation. This corresponded to the application of the as-spun draw ratio of +98% and +208%. This value was constant for each concentration of nanoadditives in the spinning solution.

The drawing process was carried out at ~ 20°C in the environment of a bath applied to the fibers after the solidification stage. Two values of the total draw ratio were used as follows: 137 and 143%. After drying on oblique rollers in 20°C, the fibers were treated with 82% ethyl alcohol for 24 h to eliminate NaCl. Completion of this process, combined with a supplementary drawing of around 5–7%, took place in 88% ethyl alcohol.

The drying process was carried out in isometric conditions on oblique rollers in 20°C. This was done to obtain the fibers which were oriented, but with a degree of crystallinity, as low as possible. This was desirable in view of the intended use of the fibers. Obtaining of such a structure was favored by conducting the drawing process below the glass transition temperature of the material and carrying out the drying stage in isometric conditions at a low temperature.

The tenacity of the fibers was determined using an Instron machine in accordance with the PN-EN-ISO 268:1997 norm.

Moisture sorption at 65 and 100% RH was determined in accordance with the PN-P-04635:1980 norm.

Total pore volume for pores in the range of 3–7500 nm and the internal surface of those pores were determined using a Carlo-Erba (Milan/Italy) mercury porosimeter connected to a computer system.

X-ray diffraction curves used in the determination of the degree of crystallinity and dimensions of crystallites were recorded using a URD6 Seifert (Ahrensburg/Germany) diffractometer with a copper target X-ray tube ($\lambda = 0.154$ nm) operated at 40 kV and 30 mA. Cu Kα radiation was monochromatized with a crystal monochromator. The WAXS curves were recorded in the 2θ range of 6°–60°, with a step of 0.1° and the registration time of 30 s per step. The fibers were cut using a microtome to eliminate texture, and then pressed into tablets with a diameter of ~ 2 cm and thickness 1 mm.

For investigation of the degree of orientation of the fibers, two-dimensional diffractograms were used. They were recorded using a diffractometer with a point collimation system (FOX2D Cu, produced by XENOCS (Sassenage/France)), which provides simultaneous collimation and monochromatization of the radiation, and a copper X-ray tube operating at the same supply parameters as those given earlier. In these investigations, the fibers were wound parallel to each other on a frame, which was then mounted in a sample holder in such a way that the primary radiation beam fell perpendicularly to the direction of the fibers. Two-dimensional diffractograms were recorded on Kodak imaging plates and read using a Molecular Dynamics scanner and Image Quant computer program.

FTIR spectra were recorded for samples made as tablets in KBr using a Jasco (Easton, Maryland) FT/IR-460 apparatus. All FTIR spectra were recorded for 32 scans in the range of 4000 cm^{-1} to 400 cm^{-1}.

RESULTS AND DISCUSSION

Analysis of the rheological parameters of the spinning solutions

The rheological parameters of a spinning solution determine its spinnability, the stability of the forming process, and avoidance of tearing of elementary fibers at the spinning nozzle. They also affect the

TABLE I
Rheological Parameters of PVA Solutions with Different Content of Nanoadditive HAp, SiO_2

Type of nanoddition	"n"	"k"
–	0.951	19,767
1% HAp	0.952	20,500
2% HAp	0.944	21,005
3% HAp	0.939	21,396
1% SiO_2	0.954	20,078
2% SiO_2	0.948	20,905
3% SiO_2	0.965	19,597

The concentration of the spinning solution was 13.2%.

course of the solidification process and the structure of the fibers produced after that stage. Analysis of the rheological properties of PVA solutions with different content of SiO_2 or HAp nanoadditive (Table I) shows that their implementation leads to strengthening of the non-Newtonian nature of the fluid. As the nanoadditive content increases, the value of the rheological parameter n decreases. Simultaneously, the parameter k, which is a measure of the consistency of the solution, goes up. An exception is the solution with 3% SiO_2 content. In this case, there was a slight increase in parameter n in comparison to the solution without nanoadditive, with the consistency of the two solutions being approximately equal.

This difference between the behavior of solutions containing 3% of SiO_2 nanoadditive and those with 3% of HAp may be due to the greater specific surface of SiO_2 and its smaller particle size than HAp. It may also be connected with the presence of urea in the solution.

Analysis of the obtained data shows that the differences between the values of the rheological parameters of solutions with 1 and 2% SiO_2 content compared with solutions containing HAp are not big. The presence of either type of nanoadditive in the spinning solution, regardless of their quantity, did not change the rheological nature of the liquid. It remained a non-Newtonian fluid, diluted by shearing, without flow boundary. The flow curves pass through the origin of the system of coordinates, and tangential stress increases less than proportionally as the shearing rate increases. An example is shown in Figure 3, for solutions with 3% content of both nanoadditives. Changes in the apparent dynamic viscosity as a function of the rate of shearing (Fig. 4) indicate the polymeric nature of the analyzed fluids. Differences in the values of the rheological parameters n and k of solutions containing 1–3% of HAp and SiO_2 nanoadditive result from mutual interactions between the polymer macromolecules, solvent molecules, and the nanoadditive. A detailed analysis of the influence of these nanoadditives on

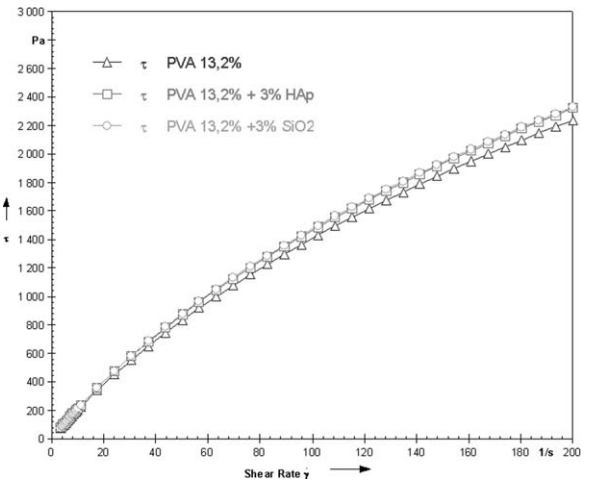

Figure 3 Flow curves for the spinning solutions used.

the mechanism of dilution by shearing was presented in our earlier publication.[11] However, this concerned a polymer of lower molecular mass, and the tested solutions did not contain urea. They also demonstrated an unsatisfactory propensity to solidify, which led us to use polyvinyl alcohol, with a higher molecular mass. To reduce the tendency of these solutions to form gel, it was necessary to add urea in a quantity determined in preliminary tests.

Analysis of the porous structure and the sorption and strength properties of PVA fibers

Analysis of the sorption properties of fibers containing different contents (from 1 to 3%) of HAp or SiO_2 nanoadditive (Table II) shows that their sorption of moisture at 65% RH lies in the narrow range: 8.7–10%. There are also only slight differences in the values of moisture sorption at 100% RH for

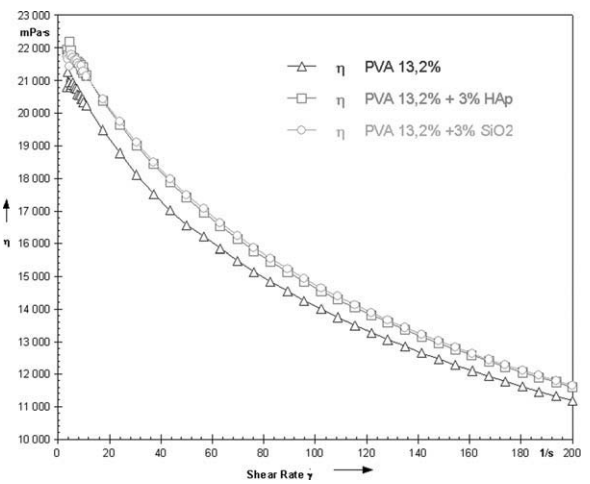

Figure 4 Apparent dynamic viscosity as a function of rate of shearing of the spinning solutions.

nanocomposite fibers regardless of the type and content of nanoadditive. The value of moisture sorption at 100% RH lies in the range of 29.7–34.29%. A similar order of magnitude for both of these parameters is obtained for fibers not containing nanoadditives. This is understandable, since the sorption properties of all of the analyzed fibers are determined by the hydrophilic nature of the material and the ability to bind water by the hydrogen bonds. The effect of total deformation on the sorption properties of these fibers is again small. The only slightly higher value of moisture sorption at 100% RH is obtained for fibers formed with a lower value of as-spun draw ratio (+98%) and 4.69 times smaller total deformation. This may be caused by the fact that these fibers' moisture sorption value at 100% RH is affected to a limited degree by the pore volume and the nature of the porous structure.

In the analysis of the porous structure, P_1 was taken to denote porosity in the range of 3–1000 nm. The value of total pore volume determined using mercury porosimetry in a range up to 7500 nm is also affected by the nonuniformity of the fiber surface (where scratches and cracks appear) and also includes the spaces between fibers which occur in the fibrous material. The total pore volume of nanocomposite fibers formed with the as-spun draw ratio of +98% varies in the range of 0.19–0.29 cm^3/g, taking higher values for fibers with a higher content (2 and 3%) of HAp or SiO_2 nanoadditive. The value of total pore volume for fibers without nanoadditive is lower, equal to 0.185 cm^3/g. A similar relationship is found in the case of P_1 porosity in a range up to 1000 nm.

For the nanocomposite fibers formed with the as-spun draw ratio of +98%, there is a high maximum within the smallest range of pores, on the distribution curve, showing the volume of pores as a function of their radius. An example is shown for fibers with 3% content of HAp and SiO_2 nanoadditive (Fig. 5). The height of this maximum in the case of fibers without nanoadditive is very low. This indicates that the implementation of HAp and SiO_2 nanoadditive into the fiber material caused formation of small, empty spaces around grains of those nanoadditives. Their presence caused high internal surface of pores in the fibers, reaching as high as 61 m^2/g. The presence of pores of these sizes is also connected with the phenomenon of moisture absorption through capillary condensation. This leads to somewhat higher moisture sorption values of nanocomposite fibers formed with the as-spun draw ratio of +98% compared with the fibers formed at the as-spun draw ratio of +201.8%.

High positive values of the as-spun draw ratio (+208%) applied at the fiber formation stage (with a similar value of the total draw ratio) cause the struc-

TABLE II
Formation Conditions, Structure, and Properties of Nanocomposite PVA Fibers

Sample's symbol	Type of nanoadditive	As-spun draw ratio (%)	Total draw ratio (%)	Linear mass (tex)	Tenacity (cN/tex)	Elongation at break (%)	Moisture sorption at 65% RH (%)	Moisture sorption at 100% RH (%)	Total volume of pores (cm^3/g)	P_1 Volume of pores 3–1000 (cm^3/g)	Total internal surface (m^2/g)
W-22	–	+98	137	33.63	7.52 ± 0.71	59.23 ± 11.00	9.07	34.98	0.1850	0.1000	11.958
W-23	–	+208	143	22.40	9.05 ± 0.92	40.88 ± 7.45	8.69	34.67	0.1698	0.0721	16.437
W-18	1% HAp	+98	137	32.67	5.79 ± 0.59	15.37 ± 4.29	9.72	31.28	0.1976	0.1566	32.103
W-19	1% HAp	+208	143	21.60	7.33 ± 0.95	16.28 ± 3.90	9.34	29.74	0.0732	0.0439	3.729
W-16	2% HAp	+98	137	32.33	7.54 ± 0.63	33.85 ± 7.09	10.00	34.29	0.2326	0.1767	31.460
W-17	2% HAp	+208	143	20.80	8.94 ± 0.55	28.73 ± 4.91	9.51	32.02	0.1186	0.0535	6.001
W-24	3% HAp	+98	137	32.03	6.19 ± 0.53	20.87 ± 4.52	9.26	29.06	0.2561	0.1659	42.748
W-25	3% HAp	+208	143	20.23	8.69 ± 1.20	24.05 ± 6.85	9.26	29.51	0.1488	0.0512	5.276
W-26	1% SiO_2	+98	137	35.16	6.90 ± 1.09	26.07 ± 7.74	9.88	28.93	0.2220	0.1683	40.706
W-27	1% SiO_2	+208	143	20.13	8.78 ± 0.98	17.59 ± 5.54	8.87	27.75	0.1279	0.0419	1.010
W-28	2% SiO_2	+98	137	33.63	5.43 ± 0.53	15.90 ± 5.40	9.03	30.48	0.2650	0.1350	51.214
W-29	2% SiO_2	+208	143	21.24	6.54 ± 0.34	13.60 ± 6.15	8.75	29.15	0.1333	0.0809	12.232
W-20	3% SiO_2	+98	137	34.47	4.98 ± 0.55	15.48 ± 5.65	9.33	29.20	0.2923	0.2512	61.448
W-21	3% SiO_2	+208	143	22.97	5.81 ± 0.79	12.23 ± 4.96	9.09	30.28	0.1116	0.0698	10.985

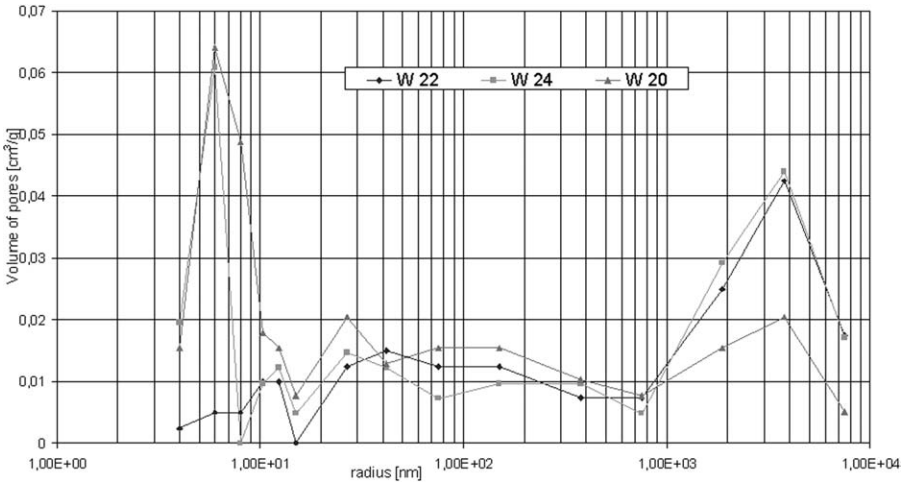

Figure 5 Volume of pores as a function of their radius for the fibers formed at the as-spun draw ratio of +98%.

tural elements to become more dense, due to the effect of the lengthwise velocity gradient. This is favored by the fact that this process takes place in a gradually solidifying stream of spinning solution. The result is a different character of the porous structure of the fibers, seen in a reduction of the quantity of pores of the smallest dimensions. There was a significant reduction in the height of the maxima corresponding to the contributions of those pores (Fig. 6). Examples are shown for fibers with 3% content of both nanoadditives. However, there was an increase in the maximum within the range of the pores with the largest dimensions, related to the porosity of the analyzed fibrous material. Such porosity is desirable in view of the role which the fibrous material will play in the biocomposite. The increase in the height of the maximum in the final range of pore dimensions for fibers formed at as-spun draw ratio of +208% is understandable in view of the significantly smaller linear density of these fibers. This is associated with the differences in total deformation. Total deformation in this case is around 7.48, compared with 4.69 for the fibers formed with the as-spun draw ratio of +98%.

Comparison of the total pore's volume values of all fibers formed at both values of as-spun draw ratio shows that the use of higher values of this parameter leads to a decrease in the porosity of the fibers. On the other hand, an increase in the content of HAp and SiO_2 nanoadditive in the fiber material is accompanied by an upward trend in their porosity.

Analysis of the strength properties (Table II) also shows that both fibers containing HAp or SiO_2 nanoadditive and fibers without nanoadditive, when formed at a higher value of the total deformation (7.48), have the tenacity which is around 2 cN/tex higher than that of fibers produced at a deformation of around 4.69 (98% as-spun draw ratio). This is understandable, as the value of this parameter is affected both by the deformation of the still liquid stream and the value of the lengthwise velocity

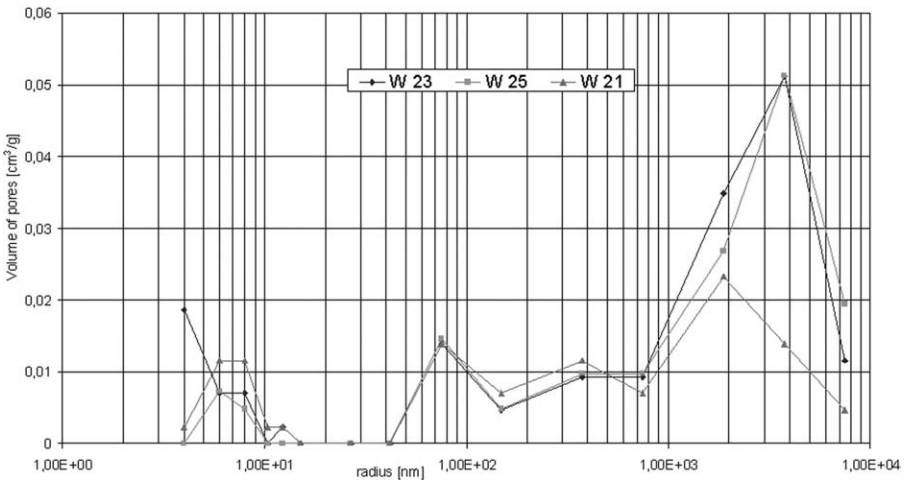

Figure 6 Volume of pores as a function of their radius for the fibers formed at the as-spun draw ratio of +208%.

gradient (dependent on the value of as-spun draw ratio), and by the amount of the deformation at the drawing stage. The higher values of the as-spun draw ratio and the deformation at the drawing stage favors better orientation of the structural elements in the direction of the axis of the fiber. Generally, for both types of nanocomposite fibers, the implementation of nanoadditive into the material led to a reduction of their strength properties. The size of these changes depends both on the type and content of the nanoadditive added to the material, as well as on the values of the as-spun draw ratio and total draw applied when the fibers were formed. In the case of fibers containing 2% of HAp for both applied values of the as-spun draw ratio, the tenacity values are similar to those of the fibers without nanoadditive: 7.5 cN/tex for fibers formed with a lower as-spun draw ratio value, and 9 cN/tex for fibers formed with a higher value. Differences in the tenacity of fibers with 1 and 3% content of this nanoadditive compared with corresponding fibers without nanoadditive are slightly greater, around 1–2 cN/tex. The implementation of SiO_2 nanoadditive into the material of the fibers causes a greater reduction in their strength properties (in comparison to the fibers without nanoadditive) than that recorded in the case of implementation of HAp nanoadditive. This is particularly visible in the case of fibers with 3% SiO_2. The different effect of the two types of nanoadditive on the strength properties of nanocomposite fibers may be a result of differences in their chemical structure. Comparing the strength properties of the two types of nanocomposite fibers, it can be assumed that the formation of secondary bonds between the OH groups of macromolecules of the polymer macromolecules and hydroxyapatite is the probable reason of their higher strength properties. This happens in spite of the greater dimensions of the HAp particles (compared with SiO_2) which make it harder for neighboring macromolecules to come together locally. Their combination with nanoadditive causes both a greater "cohesion" of the fiber material and an effective increase in the number of secondary bonds, on which in turn the strength properties of the fibers depend. Here, a 2% HAp nanoadditive content appears to be optimum. In the case of SiO_2 nanoadditive (where it is not possible for secondary bonds to form with the OH groups of the material), its presence makes it harder for macromolecules to come together and form secondary bonds. The higher the content of this nanoadditive, the clearer the effect. This happens in spite of the smaller dimensions of the grains of SiO_2.

A similar effect of the ceramic nanoadditives presence on the strength properties of the fibers has been observed for other fiber materials, such as for nanocomposite fibers made of calcium alginate.[4] The fairly low level of the tenacity for all types of obtained fibers is also due to the fact that the measurements was made at an air relative humidity of 65%. This also affected the value of the elongation at break of those fibers. High values of that parameter (40 and 50%) were obtained for fibers not containing nanoadditive. This means that they were significantly deformed during the breaking process. The implementation of HAp or SiO_2 nanoadditive into the material leads to an increase in their internal friction. This reduces the deformability of the materials, causing a decrease in the value of the elongation at break. This value still remains at a quite high level, even reaching 34% in the case of fibers with 2% HAp content.

Both the tenacity and the elongation at break of both types of nanocomposite fibers can be considered suitable from the point of view of their application in the production of a composite material. The fairly high value of the elongation at brake will not have a negative effect on the elasticity of the system as a whole. The two obtained assortments of the composite fibers (linear density of 20–22 tex and of 32–34 tex) combined with different contents of nanoadditive will be useful in the modification of the properties of the implant material.

Analysis of the results of the supramolecular structure investigations

Analysis of the WAXS diffraction curves and calculation of the degree of crystallinity and dimensions of crystallites was performed using the WAXSFIT computer program.[12] At first, a linear background was determined, based on the intensity level at small and large angles and subtracted from the diffraction curve. Moreover, the curves of all samples were normalized to the same value of integral intensity scattered by a sample over the whole range of scattering angle recorded in the experiment. Next, the experimental diffraction curves were approximated by a theoretical curve being the sum of functions representing individual crystalline peaks and an amorphous component. The curve fitting procedure was performed using a multicriterial optimization procedure and a hybrid system which combines a genetic algorithm with Powell's classical method of optimization.[13]

In this procedure, both crystalline peaks and the amorphous maxima were represented by a function being a linear combination of the Gauss and Lorentz functions. The initial angular positions of the crystalline peaks and their corresponding Miller indices were determined based on parameters of the PVA elementary cell as recorded by Bunn.[14] According to Bunn, this polymer crystallizes in a monoclinic crystallographic system, with the unit cell dimensions equal to $a = 7.81$ Å, $b = 2.52$ Å, $c = 5.51$ Å, and $\beta =$

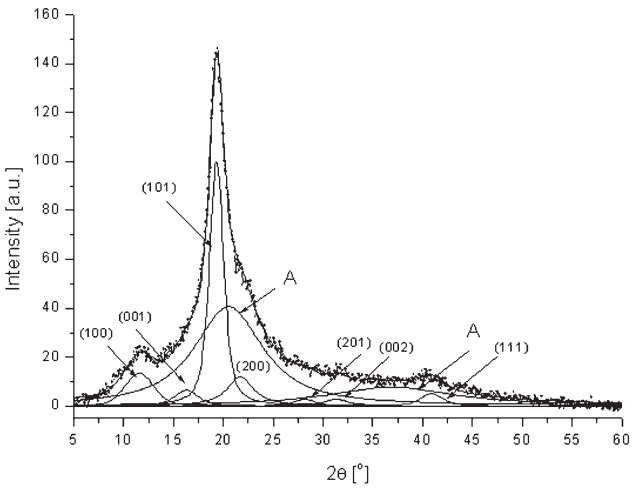

Figure 7 Diffraction pattern of PVA fibers not containing nanoadditives—sample W23. The diffraction curve is resolved into crystalline peaks and amorphous maxima.

91.7°. The edge *b* coincides with the direction of the axis of the macromolecules.

Based on this data, the interplanar distances were calculated for individual families of lattice planes, and then Bragg's law was applied to determine the angular positions (2θ) of the peaks corresponding to the given families of planes. The amorphous component was approximated using two wide maxima. One of these is localized at the scattering angle $2\theta \approx 20.5°$ and the other at $2\theta \approx 38°$.

The degree of crystallinity was calculated as the ratio of the integral intensity contained within the crystalline peaks to the integral intensity of radiation scattered by the sample over the whole measurement range (after subtraction of background radiation).

Scherrer's formula was used to calculate the dimensions of crystallites (D_{101}) in a direction perpendicular to the family of (101) lattice planes, thus in a direction perpendicular to the axis of the macromolecules. This is the origin of the strongest peak on the diffraction patterns, localized at the scattering angle $2\theta \approx 19.5°$.

An example of a diffraction pattern for a PVA fiber not containing nanoadditives is shown in Figure 7. Calculated values of the degree of crystallinity and crystallite dimensions are listed in Table III.

It can be seen that the degree of crystallinity of the investigated fibers is very similar. The differences which occur are small and do not exceed the experimental error, which is estimated at $\sim \pm 3\%$. The same is true for the crystallite dimensions, which for all of the investigated fibers are a little over 5 nm. Hence, the presence of nanoadditives in the concentrations used in this work does neither influence significantly the weight fraction nor the dimensions of crystalline regions in PVA fibers.

Figure 8 shows an example of a two-dimensional diffractogram of PVA fibers. This was recorded for the fibers W23, not containing nanoadditives, which powder pattern is shown in Figure 7.

The orientation of the fibers was estimated based on the equatorial interference arc from the (101) lattice planes—Figure 8. At the beginning, the scattered intensity distribution along the arc corresponding to those planes was found, as a function of the azimuthal angle δ: $I = I(\delta)$. The GADDS integration program was used for this purpose. The integration was carried out in the 2θ diffraction angle range: 18.0°–21.0°, which includes the (101) peak. The curves obtained were smoothed using the Microcal Origin 6.1 computer program, implemented with the Savitzky-Golay method. The azimuthal angle δ is connected with the directional angle ρ (the angle between the axis of the fiber and the normal to the given family of planes) via Polany's formula[15]:

$$\cos \rho = \cos \delta \cos \theta \quad (1)$$

where $\theta = 9.8°$, in the case of the planes considered here. Using the above equation, the function $I = I(\delta)$ was transformed into a function $I = I(\rho)$. Figure 9 shows the graph of $I = I(\rho)$ function obtained in this way for the sample W23.

Based on the obtained relationship, two parameters characterizing the orientation of crystallites in the fibers were calculated: the width at half height Δρ of the function $I = I(\rho)$ (Fig. 9) and the orientation index *k*.[16]

TABLE III
Results of the Investigations of the Supramolecular Structure of the Fibers and Their Orientation

Sample symbol	Type of nanoadditive	As-spun draw ratio (%)	Crystallinity (%)	Crystalite size $D_{(101)}$ (nm)	Δρ (°)	*k*
W-22	–	+98	38.5	5.2	48.5	0.46
W-23	–	+208	39.4	5.3	41	0.55
W-24	3% HAp	+98	38.4	5.1	47	0.48
W-25	3% HAp	+208	38.3	5.1	45	0.50
W-20	3% SiO_2	+98	39.4	5.1	42.2	0.53
W-21	3% SiO_2	+208	41.2	5.1	41.5	0.54

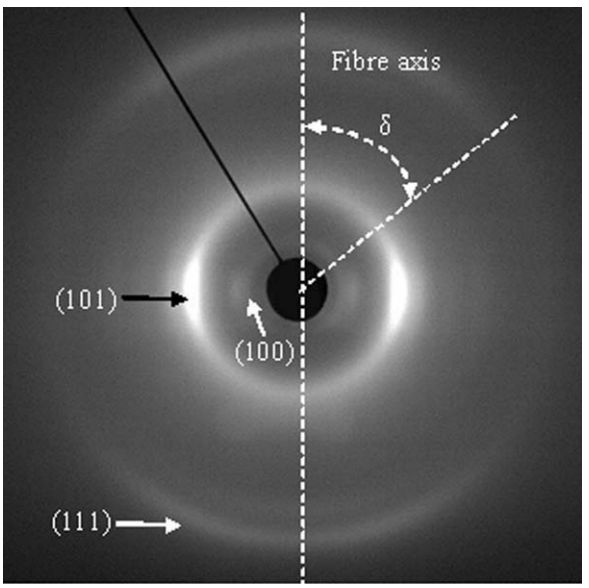

Figure 8 Two-dimensional diffraction pattern of the fibers W23. Fiber axis is vertical. The azimuthal angle δ and the equatorial interference arc from the family of (101) lattice planes are indicated in the figure.

$$k = \frac{90^o - \Delta\rho}{90^o} \quad (2)$$

The width at half height Δρ of the $I(\rho)$ function lies in between 0° (for an ideal orientation) and 90° (for a completely isotropic structure). Corresponding to this, the orientation index k takes values ranging from 0 to 1.

The calculation method described above was applied to all of the investigated fibers. The obtained results are presented in the Table III.

As it could be expected, an increase in the as-spun draw ratio causes an improvement in the orientation of crystallites in the investigated fibers.

The largest increase in orientation occurs in the fibers without nanoadditives. An increase in the as-spun draw ratio from +98% to +208% causes the orientation index k to increase significantly, reaching the highest value in comparison with other fibers. However, in fibers with nanoadditives, the increase is very slight, with the smallest changes occurring in those containing nanosilica.

This means that the presence of nanoadditives suppresses the increase in crystallites orientation which occurs as the as-spun draw ratio increases. This is an expected effect. It is interesting to note, however, that the fibers with nanoadditives have a relatively high degree of orientation—higher than that of fibers without nanoadditives—when they are formed at low values of as-spun draw ratio (+98%).

This fact suggests that the orientation of crystallites in these fibers is dependent not only on the as-spun draw ratio and the total draw ratio but also on such factors as for example the stress value during deformation.

However, the experimental data obtained in this work do not allow to give precise explanation of the observed behavior and additional investigations are necessary.

FTIR analysis of polymer and nanocomposite PVA fibers

The intended use of PVA fibers as a component of biocomposite (for implant purposes) requires a high degree of hydrolysis of the polyvinyl acetate from which the PVA is obtained. For this purpose, spectrophotometric tests were carried out on the initial polymer and on the fibers obtained from it. These tests also had the following objectives:

- to assess the differences in degree of crystallinity of the polymer and fibers;
- to determine the presence of urea (a component of the solvent) in the fibers;
- to confirm the presence of the nanoadditives HAp and SiO_2 which had been added to the fibers.

Comparing the FTIR spectra of the initial PVA [Fig. 10(a)] and of the fibers obtained from that material [Fig. 10(c)], it is observed that there is a decrease in the intensity of the band characteristic of the crystalline phase at 1141 cm^{-1}. The ratio of the height of the band of vibrations in the crystalline phase to the analytic band of vibrations of the group —CH_2— A_{1141}/A_{854} for the initial PVA is 0.959, whereas for the PVA fibers W23, it is 0.744, a result

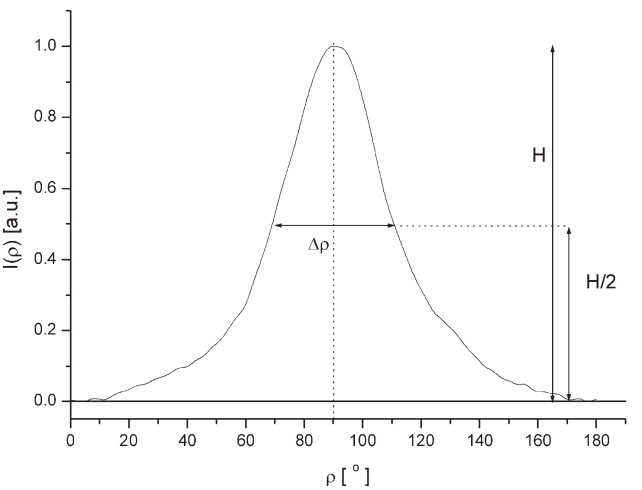

Figure 9 Normalized and smoothed scattered intensity distribution $I(\rho)$, along the equatorial interference arc produced by the (101) lattice planes, for the sample W23. The directional angle ρ is the angle between the axis of the fiber and the line perpendicular to the family of (101) planes.

which clearly indicates a lower degree of crystallinity in the PVA fibers compared with the starting mass of polymer. Comparing the FTIR spectrum of the PVA fibers W23 [Fig. 10(c)] with the spectrum for urea [Fig. 10(b)], no bands originating from urea are observed, which unambiguously indicates that the urea is fully washed out in the process of fiber coagulation.

Figure 11 shows the FTIR spectra of PVA fibers W23 (a), hydroxyapatite (b), PVA fibers W25 containing hydroxyapatite (c), nanosilica (d), and PVA fibers W21 containing nanosilica (e). In the spectrum of PVA fibers with hydroxyapatite additive [Fig. 11(c)], compared with the spectrum of PVA fibers [Fig. 11(a)], appear new bands originating from the oscillatory vibrations of the P—O bond with a maximum at 603 and 566 cm^{-1}; the presence of these bands in the FTIR spectrum of PVA fibers containing hydroxyapatite confirms the presence of nanoparticles of hydroxyapatite in the fiber mass.

Comparing the FTIR spectrum of nanosilica [Fig. 11 (d)] with the spectrum of PVA fibers W21 with nanosilica additive [Fig. 11(e)], one can observe bands located at the same or similar wavelengths; consequently, this phenomenon will cause overlapping of characteristic bands originating from nanosilica with the bands originating from PVA. The effect of the overlapping of the bands for nanosilica with those for the fiber material makes it harder to confirm unambiguously the presence of the nanoadditive in the spectrum of the PVA fibers containing nanosilica.

SUMMARY

- The hydrophilic nature of the material is a reason for the limited (small) effect of the quantity of introduced HAp or SiO_2 nanoadditive on the sorption properties of nanocomposite fibers made from polyvinyl alcohol. These properties are comparable to those for fibers not containing nanoadditive formed in analogous conditions.
- The strength properties of nanocomposite fibers formed at a constant value of total deformation depend on the quantity and type of nanoadditive. An increase in the concentration of SiO_2 nanoadditive from 1 to 3% causes a decrease in the tenacity of the fibers by 2–3 cN/tex.
- In accordance with assumptions (concerning the conditions of spinning), the nanocomposite PVA fibers obtained in this work have an oriented crystalline structure with a rather low level of crystallinity reaching 40%, and a relatively high orientation index of crystallites: 0.48–0.54. This structure, combined with a tenacity of around 8–9 cN/tex and solubility in body fluids, makes the fibers suitable as a component of implant material. The presence of HAp and SiO_2 nanoadditive in the material of the fibers will give them osteoproductive and osteoconductive properties.

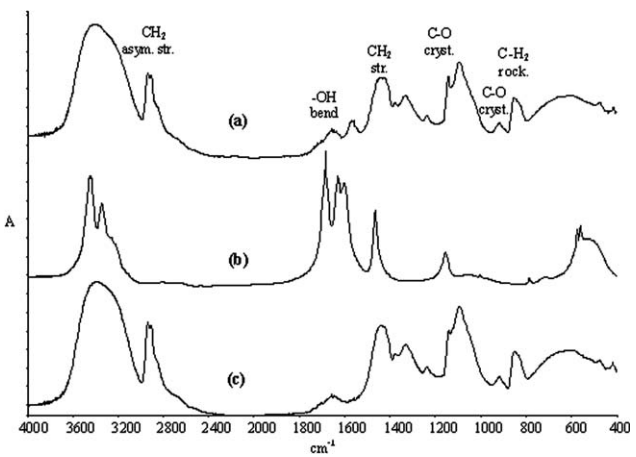

Figure 10 FTIR spectra: PVA (a), urea (b), and PVA fibers W23 (c).

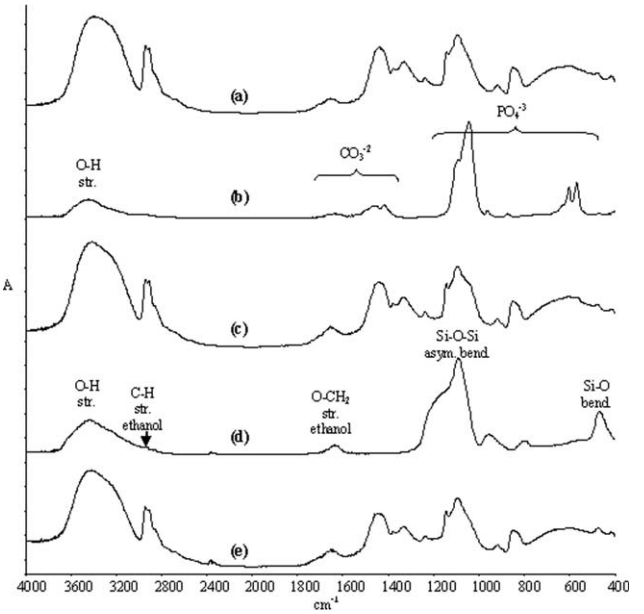

Figure 11 FTIR spectra: PVA fibers W23 (a), hydroxyapatite (b), PVA fibers W25 containing hydroxyapatite (c), nanosilica (d), and PVA fibers W21 containing nanosilica (e).

References

1. Wise, D. L. Handbook of Pharmaceutical Controlled Release Technology; Marcel Dekker: USA, 2000.
2. Zhang, C.; Yuan, X.; Wu, L.; Han, Y.; Sheng, J. Eur Polym J 2005, 41, 423.

3. Brandrup, J.; Immergut, E. H.; Grulke, E. A. Polymer Handbook; VCH: Willey, 2003.
4. Boguń, M.; Mikołajczyk, T.; Rabiej, S. J Appl Polym Sci 2009, 114, 70.
5. Mikołajczyk, T.; Boguń, M.; Kurzak, A.; Szparaga, G. Fibres Text East Eur 2009, 73, 12.
6. Fourne, F. Synthetic Fibres, Machines and Equipment, Manufacture, Properties; Hanser Publishers: Munich, 1999.
7. Rosner, T.; Wójcikiewicz, H.; Włókna syntetyczne, W. N. T. Warszawa 1969, 393.
8. Szałkowski, Z.; Poradnik inżyniera włókiennika; Wydawnictwa Naukowo-Techniczne, Warszawa 1978, 262.
9. Zhang, X.; Liu, T.; Sreekumar, T. V.; Kumar, S.; Hu, X.; Smith, K. Polymer 2004, 45, 8801.
10. Haberko, K.; Haberko, M.; Pyda, W.; Pędzich, Z.; Chłopek, J.; Mozgawa, W.; Bućko, M. M.; Sawicki, B. Sposób otrzymywania naturalnego hydroksypatytu z kości zwierzęcych; Polish Patent P-359960/2003.
11. Boguń, M.; Mikołajczyk, T. J Appl Polym Sci 2009, 114, 3452.
12. Rabiej, M.; Rabiej, S. "Analiza rentgenowskich krzywych dyfrakcyjnych polimerów za pomocą programu komputerowego WAXSFIT." Wydawnictwo ATH: Bielsko-Biała, 2006.
13. Powell, M. J. D. Comput J 1964, 7, 155.
14. Bunn, C. W. Nature 1948, 161, 929.
15. Polanyi, M. Physik 1921, 7, 149.
16. Urbańczyk, G.; Fizyka włókna, WNT Warszawa 1970, 264.